# Coherent long-time integration and Bayesian detection with Bernoulli track-before-detect

Murat Üney, *Member, IEEE*, Paul Horridge, Bernard Mulgrew, *Fellow, IEEE*, Simon Maskell, *Member, IEEE*

*Abstract*—We consider the problem of detecting small and manoeuvring objects with staring array radars. Coherent processing and long-time integration are key to addressing the undesirably low signal-to-noise/background conditions in this scenario and are complicated by the object manoeuvres. We propose a Bayesian solution that builds upon a Bernoulli state space model equipped with the likelihood of the radar data cubes through the radar ambiguity function. Likelihood evaluation in this model corresponds to coherent long-time integration. The proposed processing scheme consists of Bernoulli filtering within expectation maximisation iterations that aims at approximately finding complex reflection coefficients. We demonstrate the efficacy of our approach in a simulation example.

*Index Terms*—Bernoulli filter, coherent detection, long-time integration, staring-array radar, track-before-detect.

## I. INTRODUCTION

Detection of small and highly manoeuvrable craft with radars has been an increasingly sought after capability in many civilian and security contexts, e.g. detection of micro uncrewed air vehicles (micro-UAVs, or drones) in air traffic management [1] and small boats in maritime situational awareness applications [2], [3]. The small radar cross-sections of such objects result in very low signal-to-background and/or thermal noise ratios at the receiver array. Integration of the reflected energy over time is one of the keys to achieving a favourable detection performance in such challenging scenarios. Identification of samples to evaluate these test statistics, however, is complicated by the unknown object trajectory resulting from the manoeuvres. The fluctuations in the effective reflectivity of the object further exacerbate the aforementioned signal processing challenges.

In this work, we propose a solution which estimates the unknowns of the problem using a Bernoulli state space model; the target position, velocity and the probability of existence variables over a coherent processing interval (CPI) [4] are captured by a Bernoulli random finite set (RFS) variable [5], [6]. The state evolution over the desired integration time-window is thus modelled by a finite collection of these variables yielding a Markov chain. This model is equipped with complex radar data cube observations which are formed by using matched filtering and sampling at the receiver array front-end while illuminating the region of interest with pulse trains. We leverage on the fact that these tensor valued measurements (see, e.g. [7]) provide accurate maximum likelihood (ML) estimates of the complex valued reflectivities given their position and velocity [8].

The processing scheme we propose is an approximate inference scheme for Bayesian detection on the above mentioned model; Expectation Maximisation (EM) iterations find complex valued reflectivities within the integration time-interval for which sequential Monte Carlo (SMC) Bernoulli filtering provides the state probability density underlying the expectation. The likelihood evaluations involve complex valued radar ambiguity function evaluations at the state particles leading to coherent and adaptive processing by simultaneously digital beam-forming towards the object location and Doppler matching.

This approach can be viewed as track-before-detect [9] as signals are filtered with Bayesian recursions and not detections. State models that accommodate existence variables [5], i.e. Bernoulli state-space models [6], facilitate Bayesian detection. However, previous work in the literature builds upon non-coherent measurements (e.g. [10]) including Swerling likelihood models (see, e.g. [11]–[13]). Coherent processing for detection of manoeuvring targets, on the other hand, is often considered from a match filter design perspective (e.g. [14]–[16]) which results in combinatorial growth in the number of filters with the integration time. We use track-before-detect to circumvent this complexity in coherent long time integration using adaptive processing facilitated by Bayesian sequential inference [8]. We used this approach previously to evaluate likelihood ratio tests [17], [18] whereas this work is on Bayesian detection.

This letter is organised as follows: Section II gives the mathematical problem statement. The model underlying the proposed solution is introduced in Section III. Section IV details the proposed approximate solution and Section V demonstrates its efficacy. Finally, we conclude in Section VI.

## II. PROBLEM STATEMENT: BAYESIAN DETECTION WITH LONG TIME INTEGRATION

Let us consider the scenario in Fig. 1. A radar transmitter located at the centre of the coordinate frame illuminates a region of interest (RoI). The carrier has a wavelength of $\lambda_c$ m modulated by a train of $N$ pulses $\tilde{u}$ of duration $T_p$ and pulse repetition interval (PRI) of $T$. The emitted signal is given by

Murat Üney, Paul Horridge and Simon Maskell are with the Department of Electrical Engineering and Electronics, University of Liverpool, L69 3GJ, Liverpool, UK (e-mail: {M.Uney, P.Horridge, S.Maskell }@liverpool.ac.uk).

Bernard Mulgrew is with the Institute for Digital Communications, The University of Edinburgh, EH9 3FG, Edinburgh, UK (e-mail: B.Mulgrew@ed.ac.uk).
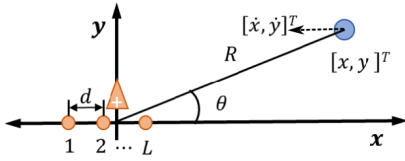
Fig. 1: A radar transmitter (triangle), receiver array (orange dots) and a reflector at $[x,y]^T$ moving with velocity $[\dot{x},\dot{y}]^T$.

$$u(t) = \mathrm{Re}\Big\{ \sum_{n=0}^{N-1} \tilde{u}(t - nT)\mathrm{e}^{j\omega_c t} \Big\}, \tag{1}$$

where $\mathrm{Re}\{\cdot\}$ denotes the real part of its complex argument.

We consider an array receiver with $L$ elements spaced by half the carrier wavelength. Each pulse induces a noisy superposition of reflections from objects in the RoI (e.g., the reflector at $[x,y]^T$ in Fig. 1) and the background. The receiver front-end signal is demodulated, matched filtered with the probing waveform $\tilde{u}$, and then sampled to obtain in-phase and quadrature-phase samples [19], without loss of generality. Associated with each pulse in the train, we denote by $\Gamma$ the number of samples output by this processing chain. All samples from the $L$ elements are often stacked as a "radar data cube" with the axis labelled as the array index (or the phase centre), pulse index (slow time) and range index (fast time) [4, Chp.3]. This acquisition scheme is illustrated in Fig. 2.

Let us stack the columns of the $r$th range bin slice in Fig. 2 to form a $LN \times 1$ data vector. This vector $\mathbf{z}(r)$ is a function of the kinematic state $\mathbf{x} \triangleq [x, y, \dot{x}, \dot{y}]^T$ which consists of the location $[x,y]^T$ and velocity $[\dot{x},\dot{y}]^T$ with $T$ denoting vector transpose. Analytic models commonly used in radar signal processing suggest that this relation takes the form

$$\mathbf{z}(r) = \begin{cases} \mathbf{n}(r), & \text{nuisance only,} \\ \alpha\,\mathbf{s}(r,\mathbf{x}) + \mathbf{n}(r), & \text{otherwise,} \end{cases} \tag{2}$$

where $\mathbf{s}$ is the received reflection model that will be detailed later in this section, and $\alpha$ is a complex number modelling the effective reflectivity (or, the reflection coefficient) assumed to remain constant during the collection of the data cube. Such time-intervals in which the effective reflectivity remains constant is referred to as a coherent processing interval (CPI) [4]. Thus, data cubes are collected in a CPI.

In (2), $\mathbf{n}(r)$ is a circularly symmetric complex Gaussian random vector with zero mean and covariance $\mathbf{\Sigma}$, i.e., $\mathbf{n}(r) \sim \mathcal{CN}(.; \mathbf{0}, \mathbf{\Sigma})$. This term captures all nuisance terms such as reflections from the background and thermal noise. The reflected signal model is

$$\mathbf{s}(r,\mathbf{x}) \triangleq \Lambda\big(rT_s - \tau(\mathbf{x}), \Omega(\mathbf{x})\big)$$
$$\times \mathbf{s}_s\big(\theta(\mathbf{x})\big) \otimes \mathbf{s}_t\big(\tau(\mathbf{x}), \Omega(\mathbf{x})\big) \tag{3}$$

$$\mathbf{s}_s(\theta) = \Big[1, \mathrm{e}^{-j\pi\sin\theta}, \dots, \mathrm{e}^{-j(L-1)\pi\sin\theta}\Big]^T, \tag{4}$$

$$\mathbf{s}_t(\tau,\Omega) \triangleq \mathrm{e}^{-j2\pi f_c\tau} \times \Big[1, \mathrm{e}^{j\Omega}, \dots, \mathrm{e}^{j(N-1)\Omega}\Big]^T, \tag{5}$$

where $\theta(\mathbf{x}) = \tan^{-1}(y, x)$, $\tau(\mathbf{x}) = 2\sqrt{x^2 + y^2}/c$, and $\Omega(\mathbf{x}) = 2\pi T/\lambda_c(\dot{x}\cos(\theta(\mathbf{x})) + \dot{y}\sin(\theta(\mathbf{x})))$ are the angle of arrival, the time-of-flight (TOF), and the angular Doppler shift, respectively, associated with $\mathbf{x}$ (Fig. 1). Here, $c \approx 3.0\mathrm{e}8$ m/s is the speed of light, $\mathbf{s}_s$ is the spatial steering vector, $\mathbf{s}_t$ is the temporal steering vector, and $\otimes$ denotes the Kronecker product
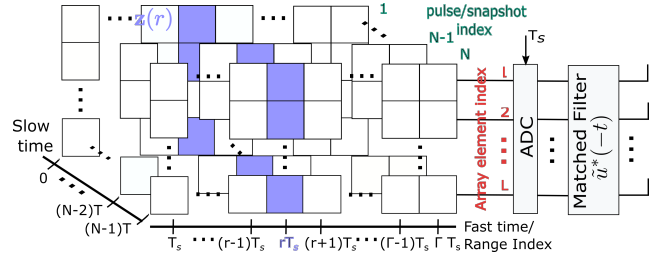


Fig. 2: Data acquisition at the receiver front-end: Demodulation, matched filtering, sampling and shift-registers.

operator. $\Lambda(\cdot)$ is the ambiguity function [20, Chp. 20] for the waveform $\tilde{u}$.

Detection via long time integration refers to taking several radar data cubes (or scans) into account before deciding on the existence of a reflector. For example, use of $K$ data cubes corresponds to integration of the reflected energy over $K \times NT$ seconds. Let us denote this data by $\mathbf{z}_{1:K}$. Existence events in $K$ steps render length $K$ Bernoulli sequences that take values from $\mathcal{T} \triangleq \{0,1\}^K$. Let us denote by $H_0 \subset \mathcal{T}$ the null hypothesis. One possible selection would contain only the all zero sequence $H_0 = \{\tau\}$ where $\tau = \mathbf{0}$ is of size $K \times 1$. Thus, detection events constitute $H_1 = \mathcal{T} \backslash H_0$. The Bayesian test for long time integration becomes

$$\frac{l(\mathbf{z}_{1:K}|H_1)}{l(\mathbf{z}_{1:K}|H_0)} \underset{H_0}{\overset{H_1}{\gtrless}} \frac{P(H_0)}{P(H_1)}, \tag{6}$$

which is equivalent to

$$P(H_1|\mathbf{z}_{1:K}) \underset{H_0}{\overset{H_1}{\gtrless}} 1/2, \tag{7}$$

$$P(H_1|\mathbf{z}_{1:K}) = \sum_{\tau \in H_1} p(\tau|\mathbf{z}_{1:K}). \tag{8}$$

The computation of the decision statistics (8) entails challenges as the events in $H_1$ have additional unknowns: The reflectivities in the signal model in (2) over $K$ CPIs, i.e., $\alpha_{1:K}$, and the state trajectory $\mathbf{X}_{1:K}$ are unknown. The rest of the article addresses these challenges in evaluating (8).

## III. BERNOULLI MARKOV MODEL WITH THE RADAR DATA CUBES

We use a Bernoulli RFS model to capture the uncertainties regarding the reflector's kinematics, i.e., $X_{1:K}$, and its existence. A Bernoulli random set $\mathcal{X}$ generates either a singleton value or an empty set; i.e. $X = \{\mathbf{x}\}$ with probability $\zeta$ and $X = \varnothing$ with probability $1 - \zeta$. Here $\mathbf{x} \sim p(.)$ is a sample from a state distribution with density $p(.)$.

The state evolution is assumed to have a first-order Markov structure and equivalently the joint probability density function of $K$ Bernoulli variables $\mathcal{X}_{1:K}$ factorises as

$$p(X_{1:K}) = p(X_1) \prod_{k=2}^{K} p(X_k|X_{k-1}), \tag{9}$$

where [6]

$$p(X_k|X_{k-1}) = \begin{cases} (1 - P_b), & X_k = \varnothing, X_{k-1} = \varnothing \\ P_b\pi_b(\mathbf{x}), & X_k = \{\mathbf{x}\}, X_{k-1} = \varnothing \\ (1 - P_s), & X_k = \varnothing, X_{k-1} = \{\mathbf{x}'\} \\ P_s\pi(\mathbf{x}|\mathbf{x}'), & X_k = \{\mathbf{x}\}, X_{k-1} = \{\mathbf{x}'\} \end{cases} \tag{10}$$

Here, $p(X_1)$ acts as the primary degree of freedom in selecting the chain's density. In the Markov transition, $P_b$ is the probability of entry of a reflector into the support of the density $\pi_b(\mathbf{x})$ which in this work is selected as a uniform density over a bounded region $\mathcal{B}$ in the state space signifying the region under test, i.e., $\pi_b(\mathbf{x}) = \mathcal{U}_{\mathcal{B}}(\mathbf{x})$ where $\mathcal{U}$ is the uniform density over $\mathcal{B}$. $P_s$ models the probability that given an object with state $\mathbf{x}'$ stays in $\mathcal{B}$ in the next step with a state transition density given by

$$\pi(\mathbf{x}|\mathbf{x}') = \mathcal{N}(\mathbf{x}; F(\Delta)\mathbf{x}', Q(\Delta, \sigma^2)), \quad (11)$$

where $F$ is a matrix that models constant velocity motion during time interval $\Delta$, and $Q$ is the process noise covariance specifying the strength of deviations via $\sigma^2$ [6].

As a result, the number of elements of $\mathcal{X}_k$, $k = 1, \cdots, K$ generate $\tau$ introduced in Section II as a sample from a Markov process with the transition matrix

$$\Pi = \begin{bmatrix} (1-P_b) & P_b \\ (1-P_s) & P_s \end{bmatrix},$$

i.e., given $X_{1:K} \sim \mathcal{X}_{1:K}$, $\tau = \big[|X_1|, \cdots, |X_K|\big]$ where $|.|$ denotes set cardinality. This chain is illustrated in Fig. 3.

The Markov model in Fig. 3 asserts the assumption that measurement uncertainties in different time steps are (mutually) independent conditioned on the state variables. The latter are related to the radar measurements through likelihoods that stem from the measurement model in (2) given by

$$l(\mathbf{z}_k(r)|X_k) = \begin{cases} l(\mathbf{z}_k(r)|\{\mathbf{x}_k\}, \alpha_k), & X_k = \{\mathbf{x}_k\} \\ l(\mathbf{z}_k(r)|\tau_k = 0), & X_k = \varnothing, \end{cases} \quad (12)$$

$$l(\mathbf{z}_k(r)|\{\mathbf{x}_k\}, \alpha_k) = \mathcal{CN}(\mathbf{z}_k(r); \alpha_k\, \mathbf{s}(r, \mathbf{x}_k), \boldsymbol{\Sigma}) \quad (13)$$

$$l(\mathbf{z}_k(r)|\tau_k = 0) = \mathcal{CN}(\mathbf{z_k(r)}; \mathbf{0}, \boldsymbol{\Sigma}). \quad (14)$$

These terms aggregate to the data cube likelihood given by

$$l(\mathbf{z}_k|X_k) = \prod_{r \in \mathcal{E}(X_k)} l(\mathbf{z}_k(r)|X_k) \prod_{r' \in \bar{\mathcal{E}}(X_k)} p(\mathbf{z}_k(r')), \quad (15)$$

where $\mathcal{E}$ is a set of samples (or range bins) associated with $X_k$ by $\mathcal{E}(X_k) = \{r|\tau(\mathbf{x}_k) \leqslant rT_p \geqslant \tau(\mathbf{x}_k) + T_p\}$. In (15), $\bar{\mathcal{E}}(X_k) \triangleq \{1, 2, \cdots, \Gamma\} \backslash \mathcal{E}(X_k)$ is the complement of $\mathcal{E}$.

Thus, the joint density of the Markov dynamic model in Fig. 3 conditioned on $\alpha_{1:K}$ is found by substituting from the above specified densities (9)–(11) and likelihoods (12)–(15) in $p(X_{1:K}, \mathbf{z}_{1:K}|\alpha_{1:K}) = p(X_{1:K}) \prod_{k=1}^{K} l(\mathbf{z}_k|X_k, \alpha_k)$. Consequently, the data posterior $p(X_{1:K}|\mathbf{z}_{1:K}, \alpha_{1:K})$ can be decomposed into the aforementioned modelling densities as well as the decision statistics in (8):

$$p(\tau|\mathbf{z}_{1:K}) = \int \mathbb{1}_\tau(X_{1:K}) p(X_{1:K}|\mathbf{z}_{1:K}, \alpha_{1:K})$$
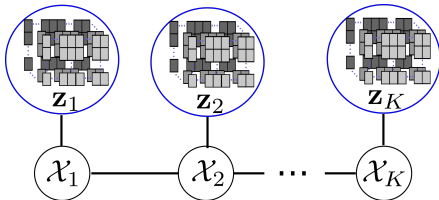$$\times\, p(\alpha_{1:K}|\mathbf{z}_{1:K}) \mathrm{d}\alpha_{1:K} \delta X_{1:K}, \quad (16)$$



Fig. 3: Dynamic system model: Bernoulli Markov model with radar data cube measurements over $K$ CPIs.

$$\mathbb{1}_\tau(X_{1:K}) = \begin{cases} 1, & |X_k| = \tau_k, k = 1, ..., K \\ 0, & \text{otherwise}, \end{cases}$$

where $\mathbb{1}$ is the indicator function, the first density inside the integral is the Bernoulli trajectory posterior, the second density is the posterior of the reflection coefficients, and the integrations above are set integrals given by $\int f(X)\delta X = f(\varnothing) + \int f(\{\mathbf{x}\})\mathrm{d}\mathbf{x}$, for Bernoulli variables.

As a result, (16) gives an explicit formula for the decision statistics in (8) using the Bernoulli Markov model detailed in this section.

## IV. APPROXIMATE INFERENCE IN THE LONG TIME INTEGRATION MODEL

Evaluation of (16) is not a straightforward computational task for both the dimensionality of the variables, the complexity of the densities and the geometry of the integration domain as determined by the indicator function involved. We propose an approximate scheme which considers first a relaxation of (16) given by

$$q(\tau|\mathbf{z}_{1:K}) \triangleq \int \Big(\prod_{k=1}^{K} \delta_{\tau_k, |X_k|}\Big) \prod_{k'=1}^{K} p(X_{k'}, \alpha_{k'}|\mathbf{z}_{1:K}) \mathrm{d}\alpha_{1:K}\delta X_{1:K}$$

$$= \int \prod_{k=1}^{K} \delta_{\tau_k, |X_k|}\, p(X_k|\mathbf{z}_{1:K}, \alpha_k) q(\alpha_k|\mathbf{z}_{1:K}) \mathrm{d}\alpha_{1:K}\delta X_{1:K}$$

where $\delta_{i,j}$ is Dirac's Delta function. Here, the joint density in (16) is approximated by the product of marginals, which is widely used in variational Bayesian inference, e.g. in mean-field approximations [21]. The Bernoulli state marginals conditioned on reflectivities can be found by Bernoulli smoothing on the model introduced in Section III. Computation of a reflectivity posterior is not straightforward, however. Let us denote the marginal existence probabilities in the above joint density by $\zeta_k$, i.e. $\zeta_k \triangleq 1 - p(X_k = \varnothing|\mathbf{z}_{1:k})$. Then,

$$q(\tau|\mathbf{z}_{1:K}) = \prod_{k=1:K} (1 - \zeta_k)^{1-\tau_k} \zeta_k^{\tau_k}. \quad (17)$$

In this work, we propose to use SMC Bernoulli forward filtering and EM to find ML estimates of reflectivities in filtering steps for approximate computation of the existence probability term $\zeta_k$ above.

### A. SMC Bernoulli track-before-detect

Bernoulli filtering on the Markov model of Section III estimates the (marginal) probability of $X_k$ taking empty set value $1 - \zeta_{k|k}$ given data cubes up to time $\mathbf{z}_{1:k}$ and reflectivity estimates $\hat{\alpha}_{1:k}$ sequentially, for $k = 1, \ldots, K$. Estimation of $\hat{\alpha}_k$s using expectation maximisation is detailed in the next subsection. Suppose for now that we are given $\alpha_{1:K}$.

The first prediction stage at $k = 1$, selects the existence probability as $\zeta_{1|0} \leftarrow P_b/(1 - P_s + P_b)$ which is the limiting probability of (12) for $X_{1|0} \neq \varnothing$. As samples generated from $\pi_b = \mathcal{U}_{\mathcal{B}}$, we use a regular grid of $P$ points over $\mathcal{B}$ (Section III) denoted by $\{\mathbf{x}_{1|0}^{(p)}\}_{p=1}^{P}$. Thus, the particle set output is $\mathcal{P}_{1|0} \triangleq \{\mathbf{x}_{1|0}^{(p)}, \omega_{1|0}^{(p)} \leftarrow 1/P\}_{p=1}^{P}$.

Let us consider prediction for $k > 1$, denote weighted samples from the previous posterior by and the existence

probability by $\hat{\zeta}_{k-1}$. The spatial predictive density based on this set is found by using the Markov transition in (10) in the Chapman-Kolmogorov equation [6] and generating a new particle set

$$\mathcal{P}_{k|k-1} \triangleq \left\{ \mathbf{x}_{k|k-1}^{(p)}, \omega_{k|k-1}^{(p)} \right\}_{p=1}^{P}. \tag{18}$$

For the case, the predicted existence probability is [6]

$$\zeta_{k|k-1} = P_b(1 - \hat{\zeta}_{k-1}) + P_s\hat{\zeta}_{k-1}. \tag{19}$$

The update at $k$ first finds the particles from the spatial posterior denoted by $\mathcal{P}_k \triangleq \{\mathbf{x}_k^{(p)}, \omega_k^{(p)}\}_{p=1}^P$ where

$$\mathbf{x}_k^{(p)} \leftarrow \mathbf{x}_{k|k-1}^{(p)}, \quad \omega_k^{(p)} = \frac{\tilde{\omega}_k^{(p)}}{\sum_{p'=1}^P \tilde{\omega}_k^{(p')}}, \tag{20}$$

$$\tilde{\omega}_k^{(p)} \triangleq L(\mathbf{z}_k|X_k = \{\mathbf{x}_{k|k-1}^{(p)}\}, \alpha_k) \, \omega_{k|k-1}^{(p)}, \tag{21}$$

$$L(\mathbf{z}_k|X_k = \{\mathbf{x}_{k|k-1}^{(p)}\}, \alpha_k) \triangleq \prod_{r \in \mathcal{E}} \frac{l(\mathbf{z}_k(r)|\{\mathbf{x}_{k|k-1}^{(p)}\}, \alpha_k)}{l(\mathbf{z}_k(r)|\tau_k = 0)} \tag{22}$$

Here, $\mathcal{E}$ is the set of all samples associated with at least one particle and the likelihoods are given in (12)–(15).

The SMC estimator for the existence probability $\zeta_k$ in the test statistics (17) is thus estimated by [6]

$$\hat{\zeta}_k = \frac{\zeta_{k|k-1} \sum_{p=1}^P \tilde{\omega}_{k|k}^{(p)}}{(1 - \zeta_{k|k-1}) + \zeta_{k|k-1} \sum_{p=1}^P \tilde{\omega}_{k|k}^{(p)}}. \tag{23}$$

The effective number of particles $\mathcal{N}_{eff}$ in $\mathcal{P}_k$ is estimated by using (51) in [22] and compared to a pre-defined threshold of $\mathcal{T}_{eff}$ to resample $\mathcal{P}_k$ when $\mathcal{N}_{eff} < \mathcal{T}_{eff}$. The spatial state of the object is estimated using the empirical weighted average of $\mathcal{P}_k$, i.e., $\hat{\mathbf{x}}_k = \sum_{p=1}^P \omega_k^{(p)} \mathbf{x}_k^{(p)}$.

### B. ML estimation of reflection coefficients

We consider the sequence of ML reflectivity estimation problems for $k = 1, \dots, K$

$$\alpha_k^{(i)} = \arg \max_{\alpha_k} \tilde{S}(\alpha_k, \alpha_k^{(i-1)}), \tag{24}$$

using EM iterations for $i = 1, 2, \dots$ which, for the Bernoulli model in Section III, yields

$$\tilde{S}(\alpha_k, \alpha_k^{(i-1)}) \propto \int L(\mathbf{z}_k|X_k = \{\mathbf{x}_{k|k-1}^{(p)}\}, \alpha_k)$$
$$\times \log L(\mathbf{z}_k|X_k = \{\mathbf{x}_k\}, \alpha_k) p(\mathbf{x}_k|\mathbf{Z}_{1:k-1}, \hat{\alpha}_{1:k-1}) \mathrm{d}x_k. \tag{25}$$

The prediction density in $\tilde{S}$ in the $k$th problem is conditioned on the estimates of the reflectivities up to time $k$, i.e., $\hat{\alpha}_{1:k-1}$. The maximiser of the Monte Carlo approximation to the expectation in (25) using $\mathcal{P}_{k|k-1}$ in (18) is found using [8]

$$\alpha_k^{(i)} =$$
$$\left( \sum_{p=1}^P \sum_{r \in \mathcal{E}(\mathbf{x}_{k|k-1}^{(p)})} \xi_k^{(p,i-1)} s(r, \mathbf{x}_{k|k-1}^{(p)})^H \mathbf{\Sigma}^{-1} s(r, \mathbf{x}_{k|k-1}^{(p)}) \right)^{-1}$$
$$\times \left( \sum_{p=1}^P \sum_{r \in \mathcal{E}(\mathbf{x}_{k|k-1}^{(p)})} \xi_k^{(p,i-1)} s(r, \mathbf{x}_{k|k-1}^{(p)})^H \mathbf{\Sigma}^{-1} \mathbf{z}_k(r) \right), \tag{26}$$

$$\xi_k^{(p,i-1)} \triangleq \omega_{k|k-1}^{(p)} \times L(\mathbf{z}_k|X_k = \{\mathbf{x}_{k|k-1}^p\}, \alpha_k^{(i-1)}) \tag{27}$$
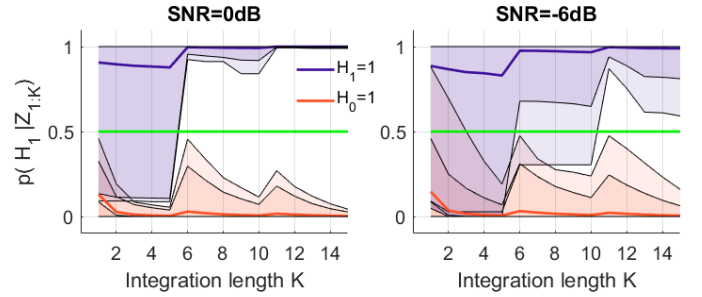


Fig. 4: Detection posteriors vs integration time: average, $\pm 3$ standard deviation and max/min posterior curves over 100 Monte Carlo experiments given one target and no target.

where the likelihood ratio in (27) is given in (22), $s$ is the reflected signal in (3), and $\mathbf{\Sigma}$ is the noise covariance in (14).

The ML estimator for $i = 1, 2, \dots$ in (26) finds projections of radar data cubes on the signal model in (3). This inner product operation on the second line of (26) diverts beams towards the (reflector) positions of $\mathbf{x}_{k|k-1}^{(p)}$s, and matches the Doppler frequencies corresponding to the velocities. Consequently, any interference from surrounding objects will be filtered out. This estimator becomes more accurate as more array elements and pulses are used (see, [8, Chp. 3]).

## V. EXAMPLE

We demonstrate the proposed Bayesian coherent long-time integration algorithm (Sec. IV) in detection of a target initially located at $[x, y]^T = [10000, 10000]^T$ m and moving towards west with 120 m/s. A mono-static radar is located at the centre (Fig. 1). $N = 250$ chirp pulses of 1 µs duration and 10 MHz bandwidth are simulated with a PRI of $T = 100$ µs in (1).

The array aperture size is $L = 128$ and the baseband sampling rate is 24 MHz yielding 25 samples per pulse at each element. The noise covariance is $\mathbf{\Sigma} = \sigma_n^2 \mathbf{I}$ where $\mathbf{I}$ is the $NL \times NL$ identity matrix. The reflectivity for each CPI is sampled from a zero mean complex Gaussian with unit variance. The per pulse signal-to-noise ratio (SNR) is thus $1/\sigma_n^2$ and the integration SNR is $N/\sigma_n^2$.

We use 100 Monte Carlo runs for very low SNRs of $0$ and $-6$ dB to demonstrate the proposed Bayesian detector; we use birth and survival probabilities of $P_b = 0.01$ and $P_s = 0.9$, respectively, with $P = 10^4$ particles initiated as a grid over the $250 \times 250$ m$^2$ cell-under-the-test centred at the initial target location and also over the velocity dimensions. Integration time lengths of $K = 1, \dots, 15$ are used; $H_0$ is the set of binary sequences with $\lfloor \sqrt{K+1} \rfloor$ elements out of $K$ being zero. Fig. 4 depicts the resulting detection posteriors (i.e. (23) in (17) and (8)) for when the target existence hypothesis $H_1$ and the null hypothesis $H_0$ is true. Increasing integration time improves the empirical detection probability (i.e. the blue region above the $0.5$ threshold) and the false alarm rate (i.e. the orange region below $0.5$ ).

## VI. CONCLUSION

In this work, we proposed a Bayesian detector capable of performing long-time integration using track-before-detect. This approach provides an adaptive and computationally feasible alternative for long-time integration and the detection of low SNR and manoeuvring objects.

## REFERENCES

[1] Carmine Clemente, Francesco Fioranelli, Fabiola Colone, and Gang Li, Eds., *Radar Countermeasures for Unmanned Aerial Vehicles*, IET, 2021.

[2] H. J. de Wind, J. E. Cilliers, and P. L. Herselman, "Dataware: Sea clutter and small boat radar reflectivity databases [best of the web]," *IEEE Signal Processing Magazine*, vol. 27, no. 2, pp. 145–148, 2010.

[3] Siqi Na, Tianyao Huang, Yimin Liu, and Xiqin Wang, "Track-before-detect for sub-nyquist radar," in *ICASSP 2020 - 2020 IEEE International Conference on Acoustics, Speech and Signal Processing (ICASSP)*, 2020, pp. 6029–6033.

[4] M.A. Richards, *Fundamentals of Radar Signal Processing*, Professional Engineering. Mcgraw-hill, 2005.

[5] Mark G. Rutten, Neil J. Gordon, and Simon Maskell, "Particle-based track-before-detect in rayleigh noise," in *Proc. SPIE*, 2004, vol. 5428, pp. 509–519.

[6] B. Ristic, Ba-Tuong Vo, Ba-Ngu Vo, and A. Farina, "A tutorial on Bernoulli filters: Theory, implementation and applications," *IEEE Transactions on Signal Processing,*, vol. 61, no. 13, pp. 3406–3430, July 2013.

[7] Dimitri Nion and Nicholas D. Sidiropoulos, "Tensor algebra and multidimensional harmonic retrieval in signal processing for MIMO radar," *IEEE Transactions on Signal Processing*, vol. 58, no. 11, pp. 5693–5705, 2010.

[8] Kimin Kim, *Reliable detection and characterisation of dim targets via track-before-detect*, Ph.D. thesis, University of Edinburgh, 2021.

[9] Y. Boers and J.N. Driessen, "Multitarget particle filter track before detect application," *IEE Proceedings Radar, Sonar and Navigation,*, vol. 151, no. 6, pp. 351–357, Dec 2004.

[10] E. Grossi, M. Lops, and L. Venturino, "A track-before-detect algorithm with thresholded observations and closely-spaced targets," *IEEE Signal Processing Letters,*, vol. 20, no. 12, pp. 1171–1174, Dec 2013.

[11] A. Lepoutre, O. Rabaste, and F. L. Gland, "Multitarget likelihood computation for track-before-detect applications with amplitude fluctuations of type swerling 0, 1, and 3," *IEEE Transactions on Aerospace and Electronic Systems*, vol. 52, no. 3, pp. 1089–1107, June 2016.

[12] Han X. Vu, Samuel J. Davey, Sanjeev Arulampalam, Fiona K. Fletcher, and Cheng-Chew Lim, "Histogram-pmht with an evolving poisson prior," in *2015 IEEE International Conference on Acoustics, Speech and Signal Processing (ICASSP)*, 2015, pp. 4060–4064.

[13] Branko Ristic, Luke Rosenberg, Du Yong Kim, Xuezhi Wang, and Jason Williams, "Bernoulli track-before-detect filter for maritime radar," *IET Radar, Sonar & Navigation*, vol. 14, no. 3, pp. 356–363, 2020.

[14] Xiaolong Chen, Jian Guan, Ningbo Liu, and You He, "Maneuvering target detection via Radon-Fractional Fourier Transform-based long-time coherent integration," *IEEE Transactions on Signal Processing,*, vol. 62, no. 4, pp. 939–953, Feb 2014.

[15] L. Kong, X. Li, G. Cui, W. Yi, and Y. Yang, "Coherent integration algorithm for a maneuvering target with high-order range migration," *IEEE Transactions on Signal Processing*, vol. 63, no. 17, pp. 4474–4486, Sept 2015.

[16] Xiaolong Li, Zhi Sun, Tat Soon Yeo, Tianxian Zhang, Wei Yi, Guolong Cui, and Lingjiang Kong, "STGRFT for detection of maneuvering weak target with multiple motion models," *IEEE Transactions on Signal Processing*, vol. 67, no. 7, pp. 1902–1917, 2019.

[17] Kimin Kim, Murat Üney, and Bernard Mulgrew, "Opportunistic synchronisation of multi-static staring array radars via track-before-detect," in *2018 IEEE International Conference on Acoustics, Speech and Signal Processing (ICASSP)*, 2018, pp. 3320–3324.

[18] K. Kim, M. Uney, and B. Mulgrew, "Coherent track-before-detect with micro-doppler signature estimation in array radars," *IET Radar, Sonar Navigation*, vol. 14, no. 4, pp. 572–585, 2020.

[19] Harry L. Van Trees, *Detection, Estimation, and Modulation Theory: Radar-Sonar Signal Processing and Gaussian Signals in Noise*, Krieger Publishing Co., Inc., Melbourne, FL, USA, 1992.

[20] M.A. Richards, J.A. Scheer, W.A. Holm, and W.L. Melvin, *Principles of Modern Radar*, Institution of Engineering & Technology, 2013.

[21] Martin J. Wainwright and Michael I. Jordan, "Graphical models, exponential families, and variational inference," *Found. Trends Mach. Learn.*, vol. 1, no. 1-2, pp. 1–305, Jan. 2008.

[22] M.S. Arulampalam, S. Maskell, N. Gordon, and T. Clapp, "A tutorial on particle filters for online nonlinear/non-Gaussian Bayesian tracking," *IEEE Transactions on Signal Processing,*, vol. 50, no. 2, pp. 174–188, Feb 2002.